Characterization of the molecular orientation in highly oriented rolled polypropylene sheets by X-ray diffraction

Claude-Paul Lafrance and Robert E. Prud'homme*

Département de Chimie and Centre de Recherche en Sciences et Ingénierie des Macromolécules, Université Laval, Sainte-Foy, Québec, Canada G1K 7P4

(Received 1 November 1993; revised 4 February 1994)

Isotactic polypropylene sheets deformed by rolling to draw ratios between 6.6 and 15.8 were studied by wide-angle X-ray diffraction. Even order $\langle P_n(\cos\chi)\rangle_c$ coefficients of the Legendre polynomial series describing the orientation distribution of the molecular chains were determined from measurements made on nine *hk*0 and *hkl* crystal planes, for *n* up to 100. The correlation between the results obtained from these different X-ray reflections is excellent. All the coefficients were used to calculate the orientation distribution of the molecular chains, which cannot be measured directly since there are no reflections parallel to the *c*-axis for the monoclinic unit cell of isotactic polypropylene. The $\langle P_2(\cos\chi)\rangle_c$ and $\langle P_4(\cos\chi)\rangle_c$ values are close to unity for the sheets rolled to $\lambda \geqslant 7.6$, indicating that the polymer chains are already well oriented in the deformation direction at these draw ratios. However, the evolution of the crystal phase orientation beyond $\lambda = 8$ can be characterized using the high-order $\langle P_n(\cos\chi)\rangle_c$ coefficients, which still increase up to the highest rolling ratio measured in this work.

(Keywords: molecular orientation; isotactic polypropylene; X-ray diffraction)

INTRODUCTION

The solid state deformation of thermoplastics by drawing, rolling or extrusion leads to a considerable enhancement of their mechanical properties in the elongation direction[1–4]. This improvement of the macroscopic properties stems from the molecular chain orientation that is induced during the processing. The characterization of the orientation at the molecular level is thus important for the understanding of the influence of the different processing parameters and for the prediction of the properties of the deformed material.

Following the pioneer work of Wilchinsky[5,6], wide-angle X-ray diffraction has been used in numerous studies aimed at the evaluation of the crystal orientation in polypropylene samples[7–14]. In most cases, the measurements were made on samples of low or moderate orientation, and the characterization of the crystal orientation was made through the determination of the $\langle P_2(\cos\chi)\rangle$ coefficient of the Legendre polynomial series distribution functions (Hermans orientation function). This coefficient gets close to its limiting value at draw ratios (λ) corresponding to the completion of the transformation from the lamellar to the fibrillar structure, usually at about $\lambda = 8$, and is constant thereafter. However, it has been shown previously that the evolution of the crystal orientation distribution of polyethylene samples drawn to λ as high as 50 can be described through the high-order coefficients of the Legendre polynomial series[15,16]. In this study, the molecular orientation of isotactic polypropylene (i-PP) sheets deformed by roll-drawing to draw ratios over 6 was investigated by wide-angle X-ray diffraction. The $\langle P_n(\cos\chi)\rangle_c$ coefficients relative to the molecular chain orientation were determined for *n* up to 100 from nine different *hk*0 and *hkl* crystal planes of the monoclinic unit cell of i-PP. The orientation distribution of the molecular chains, which cannot be measured directly because of the absence of crystalline reflection parallel to the carbon backbone, was then calculated by using a series expansion of the Legendre polynomial distribution function.

EXPERIMENTAL

Samples

The isotactic polypropylene samples investigated in this study were prepared by uniaxial rolling in the laboratory of Dr Raymond Woodhams (University of Toronto, Ontario, Canada)[17,18]. Transparent oriented sheets were obtained by single-pass rolling at 158°C of commercial sheets made of Trovidor 500 resin (Dynamit Nobel Ltd, $M_n = 70\,000$, $M_w = 377\,000$). The preheated 10 mm thick billets were first rolled to a thickness of approximately 1 mm by passing through a set of work rolls, and the overall deformation ratio was then achieved by operating three pairs of traction rolls at higher rotational speeds than the feed rolls[18]. The uniaxially oriented sheets had deformation ratios of 6.6, 7.6, 8.2, 9.6, 14.6 and 15.8, with thicknesses ranging from 1.45 to 0.70 mm.

* To whom correspondence should be addressed

0032-3861/94/18/3927-09

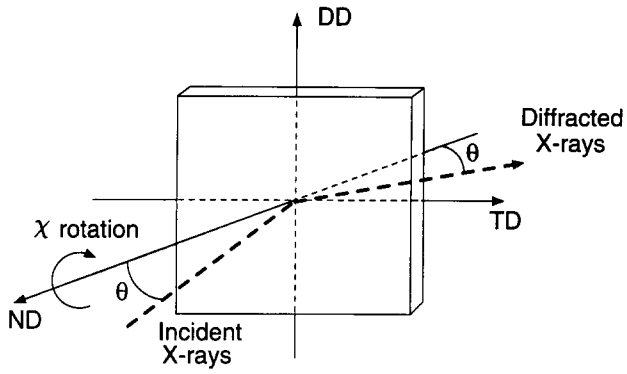

Figure 1 Experimental set-up for orientation measurements by wide-angle X-ray diffraction using the symmetrical transmission geometry; DD: deformation direction; TD: transverse direction; ND: normal direction

X-ray measurements

Wide-angle X-ray diffraction measurements were made using nickel-filtered Cu Kα radiation (0.154 178 nm) produced by a Rigaku rotating anode X-ray generator (Rotaflex RU-200BH) operated at 55 kV and 190 mA. The collimation of the incident beam was achieved using a Soller slit and a 1.0 mm pinhole and the detection of the diffracted intensity was provided by a scintillation counter coupled with a pulse-height analyser. The geometry of the experimental set-up is shown in *Figure 1*. All curves were recorded with the symmetrical transmission technique, the normal to the sample surface being positioned at an angle θ with respect to the incident X-ray beam and the detector at an angle 2θ. For the orientation measurements, the polar angle (χ) defining the rotation of the sample around the normal to its surface was rotated from $-90°$ to $90°$ by $0.5°$ steps, $\chi=0°$ corresponding to the rolling direction. The instrumental broadening was limited by using $1.0°$ and $0.5°$ receiving slits for the 2θ and χ angle resolution, respectively.

Calculations

The complete characterization of the molecular orientation in a polymer sample involves the determination of its orientation distribution, $N(\chi, \phi)$, which can be obtained by X-ray pole figure measurements. For uniaxially oriented polymer samples, the orientation distribution of a given structural unit often exhibits cylindrical symmetry about its deformation direction. The orientation distribution then reduces to $N(\chi)$, and it can be represented by a series in even terms of Legendre polynomials, $P_n(\cos\chi)$[1,2,19]:

$$N(\chi)=\sum_{n=0}^{t}(n+\tfrac{1}{2})\langle P_n(\cos\chi)\rangle P_n(\cos\chi) \qquad (1)$$

where the brackets indicate that the $\langle P_n(\cos\chi)\rangle$ coefficients are obtained by taking an average over all the orientations in the sample. Only the even $\langle P_n(\cos\chi)\rangle$ values are necessary for the characterization of the crystal plane orientation, since the odd coefficients are equal to zero for reasons of symmetry[1]. For unoriented samples, all coefficients are equal to zero, except the zeroth order coefficient, which is equal to unity. For a perfect orientation of the structural units in the deformation direction, all the coefficients would be equal to unity.

In this work, the $\langle P_n(\cos\chi)\rangle$ coefficients, with $n=2$–100, were calculated from the distribution of the diffracted X-ray intensity measured in polar scans of nine different crystal planes by using the equation[1,2,19]:

$$\langle P_n\rangle \equiv \langle P_n(\cos\chi)\rangle = \frac{\int_0^{90} I^*(\chi)P_n(\cos\chi)\sin\chi\,d\chi}{\int_0^{90} I^*(\chi)\sin\chi\,d\chi} \qquad (2)$$

The corrected intensity, $I^*(\chi)$, was obtained by subtracting the background intensity value from the sum of the two measurements made at $-\chi$ and $+\chi$. The background was evaluated by two different methods. For the samples with $\lambda=6.6$, 7.6 and 8.2, the background was taken as the minimum intensity read at the 2θ peak position on baselines drawn in Bragg angle scans measured at different polar angles. At higher draw ratios, the former procedure was found to give background values identical to the minimum intensity measured in the polar scans of the different reflections, and the latter values were used in the calculations.

The $P_n(\cos\chi)$ polynomials were obtained by using the recurrence relation[20]:

$$(n+1)P_{n+1}(\cos\chi)=(2n+1)\cos\chi P_n(\cos\chi)-nP_{n-1}(\cos\chi) \qquad (3)$$

using $P_0(\cos\chi)=1$ and $P_1(\cos\chi)=\cos\chi$ as the initial values. The numerical integration of equation (2) was performed using Simpson's rule. The upper calculation limit ($n=100$) was chosen in order to obtain a good fit between the experimental orientation distribution measured for the $\lambda=15.8$ sample and the distribution reconstructed through equation (1).

It is general practice in polymer crystallography to set the c-axis parallel to the direction of the molecular chains. For polymers which possess crystal reflections parallel to the c-axis, the coefficients describing the molecular orientation can be obtained directly from X-ray measurements as has been done, for example, for the 002 crystal planes of highly oriented polyethylene[15,16,21,22]. However, this is not possible for i-PP, which has a monoclinic unit cell. Nevertheless, if the crystal orientation exhibits cylindrical symmetry with respect to the deformation direction, the Legendre polynomial coefficients relative to the molecular chains, $\langle P_n\rangle_c$, can be determined from the coefficients measured from any hkl crystal plane, $\langle P_n\rangle_{hkl}$, by using the equation[15,23]:

$$\langle P_n\rangle_c=\langle P_n\rangle_{hkl}/P_n(\cos\phi_{hkl}) \qquad (4)$$

where ϕ_{hkl} is the angle between the normal to the hkl plane and the c-axis.

RESULTS AND DISCUSSION

Crystal planes of interest

Table 1 lists the 2θ and ϕ angles for the different crystal planes that were investigated. The monoclinic unit cell parameters, $a=0.667$ nm, $b=2.084$ nm, $c=0.6495$ nm, $\beta=99.33°$, were obtained by starting with the values given in the literature for the α-form of i-PP[5,24,25] and then optimizing the fit between the calculated and experimental 2θ position of 15 different reflections.

For all samples, the measurements showed that the orientation distribution of the different crystal reflections were centred at the ϕ angle defining their inclination with

Table 1 Experimental and calculated values (in degrees) of the Bragg angle (2θ) and the angle ϕ between the *hkl* plane normal and the *c*-axis, for different isotactic polypropylene crystal reflections (monoclinic unit cell, α form, $a=0.667$ nm, $b=2.084$ nm, $c=0.6495$ nm, $\beta=99.33°$)

	Calculated		Experimental	
hkl	2θ	ϕ	2θ ±0.02	ϕ ±0.5
110	14.11	90.0	14.10	90.0
040	17.02	90.0	17.02	90.0
130	18.57	90.0	18.57	90.0
111	21.29	50.0	21.20	50.0
$\bar{1}31$	21.86	51.2	21.99	51.3
041	21.99	51.5		
022	29.16	19.4	29.21	19.3
$\bar{1}12$	29.27	20.0		
$\bar{1}13$	42.54	11.0	42.56	10.9

respect to the *c*-axis. This result indicates that the molecular chains are aligned in the rolling direction, as can be expected for samples deformed to such high draw ratios.

Figure 2 presents Bragg angle scans taken at polar angles of 0°, 20°, 50° and 90° for the $\lambda=8.2$ oriented PP sheet, while *Figure 3* shows polar scans measured, for the $\lambda=7.6$ sheet, for the different crystal planes that were studied. It is observed in the $\chi=90°$ diffractogram (*Figure 2*) that the 110, 040 and 130 planes give rise to intense and well resolved diffraction peaks superposed on the amorphous halo. The background intensity determinations made on Bragg angle scans of the different samples show that this halo orients toward the equator ($\chi=90°$). Thus, for highly oriented polypropylene samples, the background cannot be considered as independent of χ in the range $2\theta=10°$–$25°$. This orientation of the amorphous halo could interfere in the crystal orientation calculations, although its weak intensity with respect to the three intense *hk*0 crystalline peaks indicates that the effect should be small.

The amorphous component appears as a shoulder at the bottom of the 110, 040 and 130 polar peaks drawn on a reduced intensity scale in *Figure 3*. These curves also indicate the presence of weak unresolved crystalline reflections, namely that from the $\bar{1}11$ crystal plane in the 130 scan and contributions from the 021 and $\bar{1}11$ planes in the 040 scan. There is a peak located at $\chi\approx10°$ in the 110 polar scan of all samples rolled to $\lambda\leqslant9.6$, which is absent in the scans measured at higher deformation ratios. This crystal reflection can also be observed at approximately $2\theta=14°$ in the diffractograms taken at $\chi=0°$ and 20°, whereas the diffracted intensity of the 110 reflection should be negligible at these polar angles. Considering the unit cell of the α-form of i-PP, this peak has to be indexed as the 001 reflection, which is oriented at $\phi=9.3°$ with respect to the *c*-axis. However, this reflection should be absent for symmetry reasons according to the space group that has been assigned to this crystal form. This peak cannot be indexed as a reflection of either the β or γ form of i-PP. Therefore, it is proposed that the deformation of the polymer causes some disorder in the crystals, thus reducing the symmetry which normally precludes the appearance of the 001 reflection. A similar explanation has been proposed to account for the appearance of the 001 reflection in highly oriented polyethylene samples, which is normally absent from the diffraction pattern[15,16].

The 111 and $\bar{1}31$/041 crystal planes were used to determine the molecular orientation despite the fact that their diffraction peaks overlap (*Figure 2*, $\chi=50°$). In the experimental conditions that were used for the measurement of the polar scans, the contribution of the unresolved component should be small. Moreover, since these reflections are oriented at ϕ angles that differ by 1° only (*Table 1*), it was assumed that the broadening of the orientation distribution caused by the overlapping component could be neglected. Finally, in the case of the 022/$\bar{1}12$ and $\bar{1}13$ crystal planes, the orientation distribution measurements presented in *Figure 3* show that the unresolved reflections are sufficiently separated from the peak of interest to be removed by the curve-fitting procedure described below.

Removal of unresolved contributions

Two procedures can be used to remove the contribution of non-resolved components in polar scans prior to orientation calculations. If the diffracted intensity of the crystal plane of interest falls to the background value before the onset of the other components, then $\langle P_n\rangle$ calculations can be made on a limited angular range. This procedure is mostly useful with highly oriented samples, where the different reflections measured in a polar scan show up as narrow and well separated peaks. For polyethylene samples extruded to draw ratios between 6 and 20, it was shown that an excellent agreement is obtained when this method is used to calculate the $\langle P_n\rangle_c$ coefficients from different *hk*0, *hkl* and 00*l* crystal planes[15].

A second method involves curve fitting of the experimental distribution and conducting the orientation calculation on the function corresponding to the peak of interest[16]. In this study, a Pearson VII function was used to fit the polar scan peaks:

$$P(\chi)=I_0/\{1+4[(\chi-\chi_0)/a]^2(2^{1/m}-1)\}^m \quad (5)$$

where I_0 is the maximum intensity, χ_0 is the peak position, whereas *a* and *m* are factors controlling, respectively, the width of the peak and the shape of the tail of the distribution. This function gives excellent results for the approximation of X-ray diffraction peaks measured in either 2θ[26,27] or χ[16,28] scans. The quality of the correlation between the experimental curve, $N(\chi)$, and the calculated distribution, $P(\chi)$, was evaluated by the error function:

$$\sigma=\sum[N(\chi)-P(\chi)]^2/\sum N(\chi)^2 \quad (6)$$

For all curves, σ values smaller than 0.15% were obtained in the full angular range from $\chi=0°$ to 90°, whereas the fitted curves gave $\sigma<0.08\%$ for a region of 15° from the peak maximum.

Table 2 gives selected $\langle P_n\rangle_c$ values for the $\lambda=8.2$ sheet, calculated either from the experimental curves or from the Pearson VII distributions, for the 110, 040 and 130 reflections and the average values obtained for the *hkl* reflections. It is observed that the $\langle P_2\rangle_c$ coefficients obtained directly from the measured distribution for the 040 and 130 reflections are smaller than the results calculated from other crystal planes. This difference cannot be ascribed solely to contributions from the weak 021 and $\bar{1}11$ reflections, which show up at about $\chi=35°$–$40°$ on the polar scans of the 040 and 130 crystal

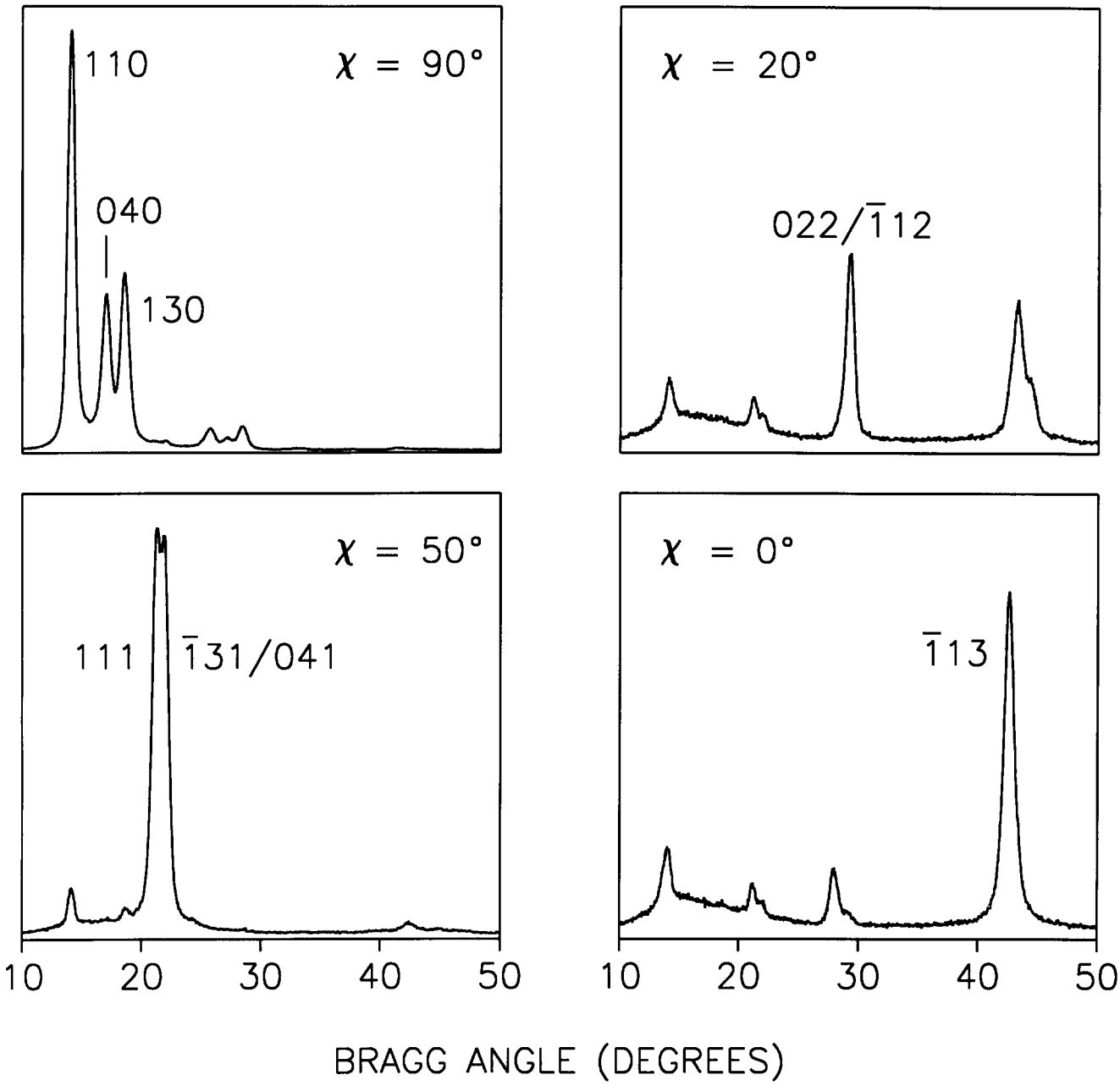

Figure 2 Bragg angle scans measured for the $\lambda = 8.2$ rolled polypropylene sheet at the specified polar angles. The relative intensity scales are the following: 1 for $\chi = 90°$, 1/3 for $\chi = 50°$ and 1/6 for $\chi = 20$ and 10°

planes (*Figure 3*), but also to a broadening of the polar peaks arising from the orientation of the amorphous halo, which is oriented toward the plane perpendicular to the deformation direction (ND–TD plane, *Figure 1*). Since the halo has its maximum intensity at around $2\theta = 18°$, the amorphous contribution affects mostly the measurements made for the 040 and 130 crystal planes, although the $\langle P_2 \rangle_c$ coefficient calculated for the 110 plane is also slightly decreased by the broadening, as compared to the value obtained from the *hkl* planes.

The higher order coefficients are less affected by the amorphous contribution, because of the shape of the corresponding $P_n(\cos \chi)$ polynomial curves that change sign $n/2$ times between $\chi = 0°$ and 90°. For broad distributions, a summation of alternating positive and negative areas then gives a numerator value close to zero in equation (2). Thus, the broad amorphous component does not contribute significantly to high $\langle P_n \rangle$ coefficients, which depend rather on the position and shape of narrow peaks in orientation distribution measurements.

The results presented in *Table 2* demonstrate that an excellent agreement is obtained between the coefficients calculated for the different crystal planes by using the Pearson VII approximation of the measured orientation distributions. The correlation between the $\langle P_n \rangle_c$ values obtained from all reflections investigated is shown in *Figure 4*, which shows the variation of these coefficients as a function of n, for the samples with $\lambda = 6.6$ and 14.6. These curves exhibit a typical S shape, as has been reported previously for extruded rods and for drawn films of polyethylene[15,16]. The coefficients calculated from *hk*0 reflections decrease smoothly with n, while those obtained from *hkl* planes are somewhat scattered on both sides of the curve defined by the former coefficients. This scatter is a consequence of the shape of the Legendre polynomials: when the ϕ angle between the centre of the

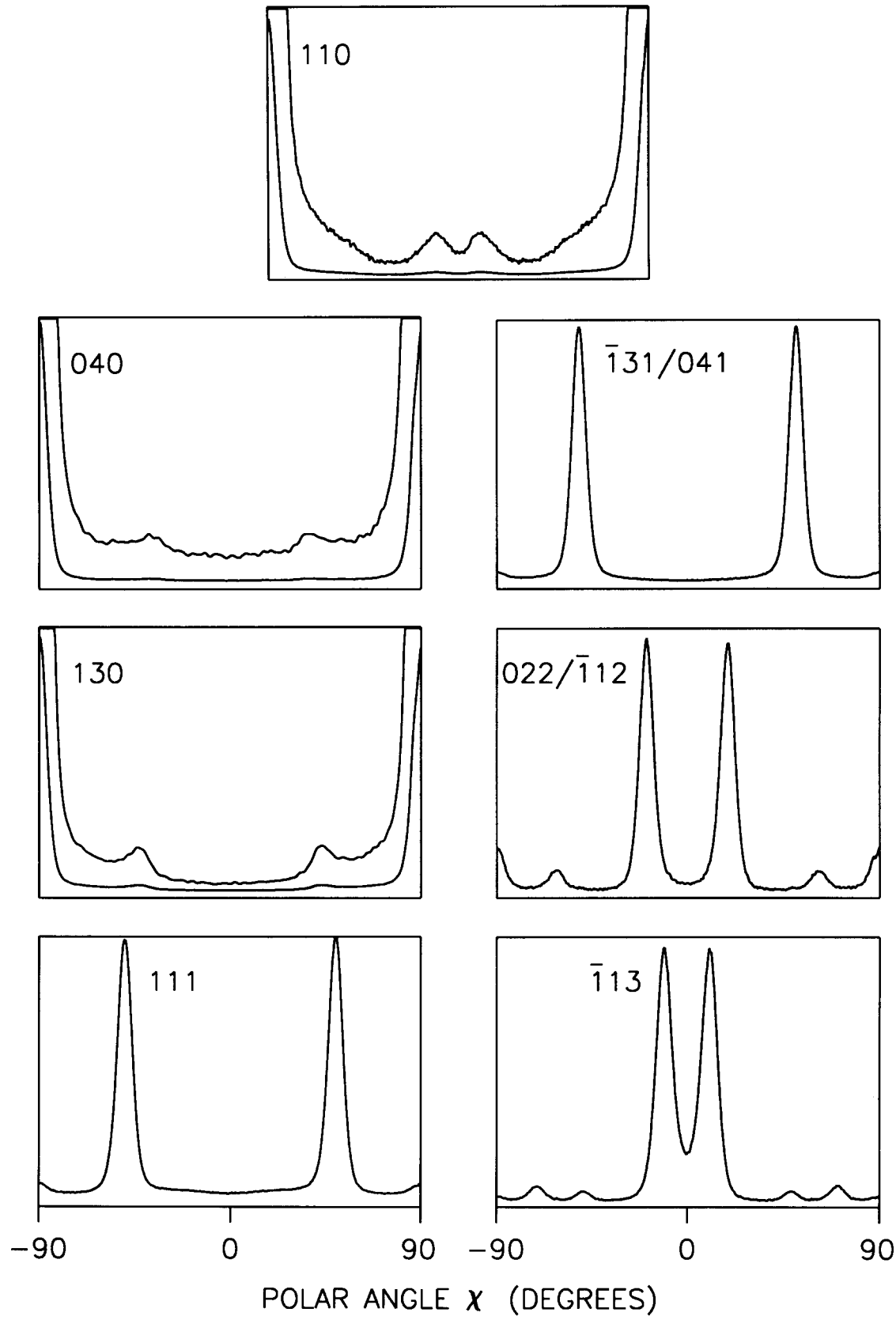

Figure 3 Polar angle scans measured for the $\lambda = 7.6$ rolled polypropylene sheet for seven different crystal planes. The scans of the 110, 040 and 130 reflections are also drawn on a reduced intensity scale to emphasize the presence of weak unresolved contributions from other crystal planes

orientation distribution and the molecular chain axis corresponds to a $P_n(\cos\phi)$ value close to zero, a considerable uncertainty is generated for the $\langle P_n \rangle_c$ coefficient calculated using this small denominator in equation (4)[15]. For example, for several samples, $\langle P_2 \rangle_c$ values above unity were calculated from the experimental curves of the 111 and $\bar{1}31/041$ crystal planes. Since the value of the $P_2(\cos\chi)$ polynomial is zero at 54.7°, these reflections, oriented at approximately 50° from the deformation direction, are not suitable to

obtain significant results for the second-order coefficient. Nevertheless, the correlation between the $\langle P_n \rangle_c$ coefficients obtained from the different reflections after the curve fitting procedure is excellent.

In accordance with the preceding results, Unwin *et al.*[13] have reported that a good agreement is obtained between the second- and fourth-order orientation coefficients determined from the 110, 040, 130 and $\bar{1}13$ reflections of i-PP. Furthermore, they showed that the $\langle P_2 \rangle_c$ and $\langle P_4 \rangle_c$ coefficients calculated for drawn films of i-PP do not agree with the values predicted by the pseudo-affine deformation model proposed by Kratky, which assumes that the material can be represented by a two-phase structure where the crystal domains orient as rigid rods embedded in a softer amorphous matrix[1]. The curves corresponding to the coefficients calculated from this model, for draw ratios of $\lambda = 6.6$ and 14.6, are presented in *Figure 4* (broken curves); their shape is different from that of the experimental results, which confirms the conclusion of Unwin *et al.* At draw ratios above 6, the molecular orientation distribution calculated using the pseudo-affine deformation scheme shows a sharp peak centred in the deformation direction, with a tail that decreases slowly toward zero. This latter population of crystals, oriented away from the deformation axis, yields small values of the low-order $\langle P_n \rangle_c$ coefficients, as is observed at $\lambda = 14.6$ in *Figure 4*. Yet, as stated previously, the high-order $\langle P_n \rangle_c$ coefficients depend mostly on the presence of narrow peaks in the orientation distribution, and the sharp component of the pseudo-affine distributions explains the fact that their curves in *Figure 4* are located above the experimental curves at high n values.

Table 2 Selected $\langle P_n \rangle_c$ coefficients calculated directly from the experimental orientation distributions and from Pearson VII fitted distributions of the 110, 040 and 130 reflections, and average values obtained from the 111, $\bar{1}31$/041, 022/$\bar{1}22$ and $\bar{1}13$ reflections (hkl_{av}) for the $\lambda = 8.2$ rolled sheet

	Experimental curves				Pearson VII curves			
n	110	040	130	hkl_{av}	110	040	130	hkl_{av}
2	0.95	0.91	0.87	0.97	0.98	0.98	0.98	0.97
18	0.43	0.42	0.39	0.45	0.46	0.47	0.47	0.46
34	0.11	0.12	0.11	0.13	0.11	0.12	0.12	0.13
50	0.01	0.01	0.01	0.02	0.01	0.02	0.02	0.03

Occurrence of double orientation

It has been reported by many workers that the deformation of polypropylene induces double orientation of the crystal phase. Pole figure measurements made by Wilchinsky[6], and by Dhingra *et al.*[11], showed that cold rolling produces an oriented structure where the c-axis is aligned in the deformation direction whereas the b-axis concentrates towards the normal to the film surface. Okajima and Homma[8], and Shankernarayanan[14] observed a similar orientation behaviour of i-PP deformed at temperatures over 140°C by drawing and by roll-drawing, respectively. However, Shimomura *et al.* reported that double orientation occurs in tubular film extrusion when the specimens are biaxially oriented, but not in the case of uniaxially oriented films[12].

In order to determine if double orientation is present in the rolled sheets, measurements of the distribution of the 110 and 040 reflections in the normal–transverse plane were made by rotating the samples around

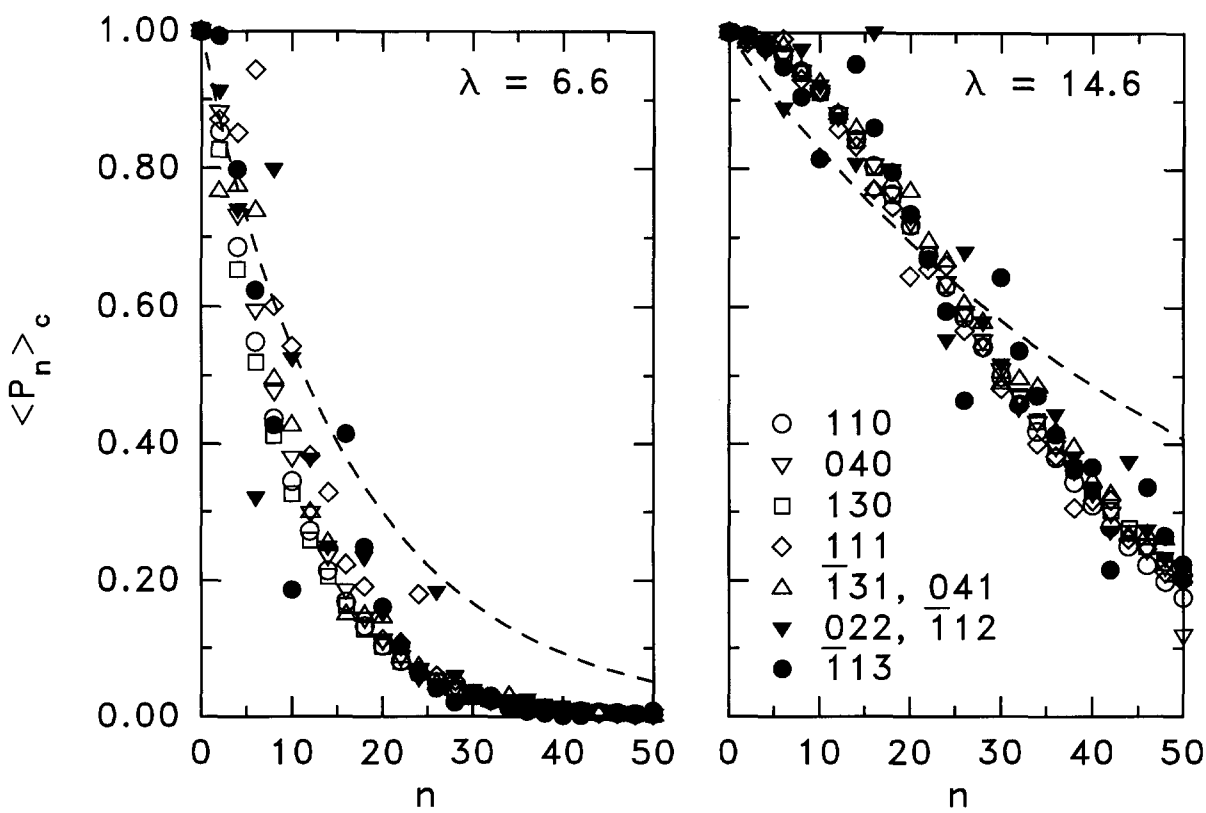

Figure 4 $\langle P_n \rangle_c$ coefficients calculated from the Pearson VII fitted distributions of the different crystal planes as a function of n, for the rolled polypropylene sheets with $\lambda = 6.6$ and 14.6. (– – –) Coefficients calculated from the pseudo-affine deformation model (see text)

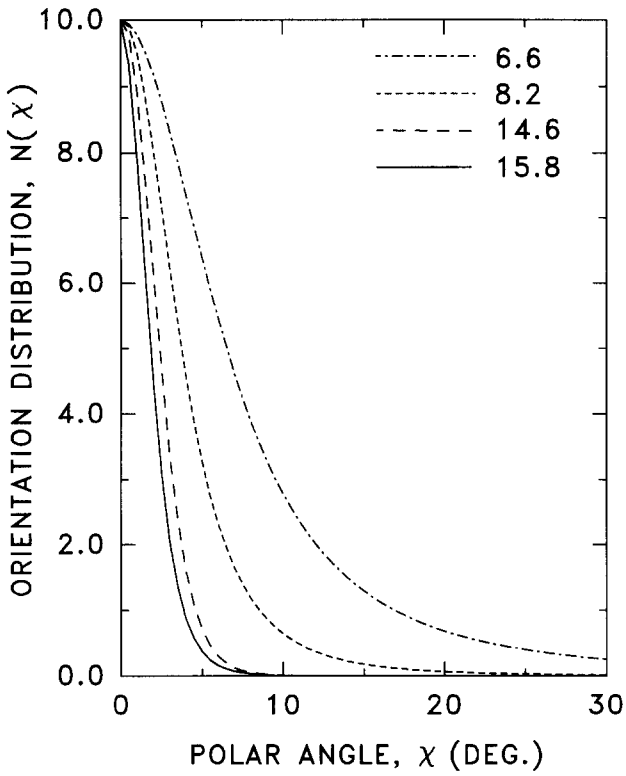

Figure 5 Orientation distribution of the molecular chains calculated from average $\langle P_n \rangle_c$ coefficients ($n \leqslant 100$) for polypropylene sheets of different draw ratios, λ

their deformation direction. For the 110 plane, these measurements showed broad distributions approximately centred in the transverse direction, whereas the 040 scans indicate that the *b*-axis aligns preferentially toward the direction normal to the sheet surface, in accordance with the observations described in the preceding paragraph. The double orientation was found to increase with the draw ratio, although this effect is not very pronounced even at $\lambda = 15.8$. The low development of the double orientation in the samples explains the fact that the shape of the three intense *hk*0 peaks measured in the Bragg angle scans ($\chi = 90°$) compares so well with the diffractometer curves reported by Shankernarayanan[14], by Natta and Corradini[24] and by Turner-Jones *et al.*[25] for unoriented i-PP. In the case of X-ray measurements made by symmetrical transmission (*Figure 1*), only the crystal planes oriented approximately parallel to the DD–ND plane contribute to diffraction, and a weakening of the intensity of the 0*k*0 reflections would result from the orientation of these planes towards the DD–TD plane (*b*-axis aligned along ND).

In addition, a considerable decrease in intensity of the 040 reflection caused by a strong double orientation would lower the $\langle P_n \rangle_c$ coefficients obtained for this crystal plane as compared with those calculated from reflections oriented toward the transverse direction, which is not observed for the samples studied in this work (see *Table 2* and *Figure 4*). In the case of doubly oriented drawn films of polyethylene, important discrepancies have been reported to arise between the Legendre coefficients derived from different *hk*0 planes[16]. The excellent agreement between the $\langle P_n \rangle_c$ results calculated from the different i-PP crystal planes indicates that the high-temperature rolling process used to prepare the thick oriented sheets induces only weak double orientation. Thus, this small deviation from cylindrical symmetry does not preclude the use of the Legendre polynomial representation of the orientation (equations (1)–(3)), instead of the spherical harmonics analysis required in complex orientation cases.

Evolution of the molecular orientation

The average $\langle P_n \rangle_c$ coefficients obtained from all crystal planes investigated can be used in equation (1) in order to calculate the molecular chain orientation distribution, $N(\chi)_c$, which is given in *Figure 5* for sheets of different draw ratios. Coefficients with n up to 100 were required to obtain smooth $N(\chi)_c$ distributions for the more highly oriented samples, since the termination of the series at $\langle P_n \rangle_c$ values which are not close to zero introduces oscillations in the low-density regions of the curves[15,19]. *Figure 5* shows that the molecular chain orientation distribution narrows down with increasing draw ratio, and this variation is still significant at $\lambda > 15$. It is also observed that a significant fraction of chains is still oriented at $\chi \geqslant 30°$ at $\lambda = 6.6$, even if a $\langle P_2 \rangle_c$ value near 0.9 is obtained at this draw ratio. The width of the orientation distribution decreases markedly between this latter sample and the sheets deformed at $\lambda = 7.6$ and 8.2, where almost all the molecular chains are oriented at angles within 20° of the rolling direction. This narrowing of the molecular chain orientation distribution is shown more clearly in *Figure 6*, where the full-width at half-height of the distribution, $\chi_{1/2}$, is plotted as a function of λ.

It can be observed in *Figure 7* that the evolution of the orientation of the crystal phase at high draw ratios cannot be characterized by the $\langle P_2 \rangle_c$ coefficient, which

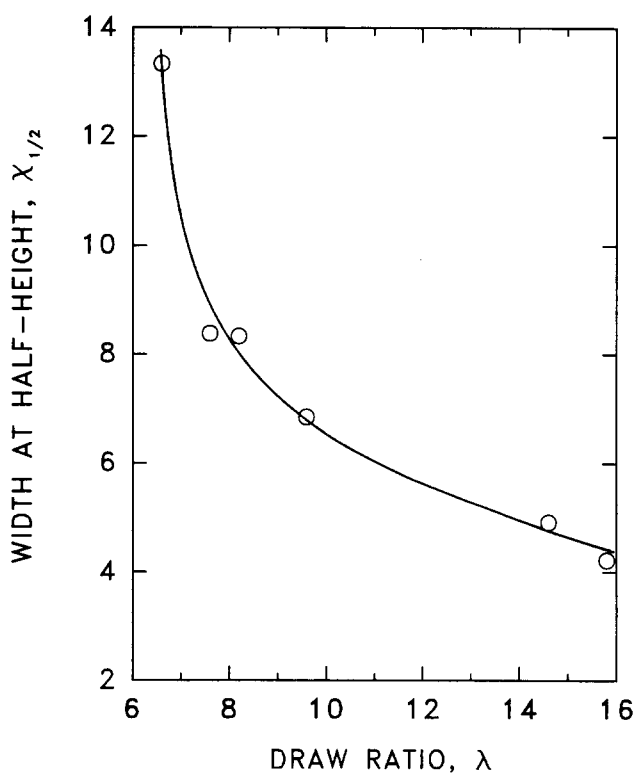

Figure 6 Width at half-height of the molecular chain orientation distribution as a function of draw ratio for roll-drawn polypropylene sheets

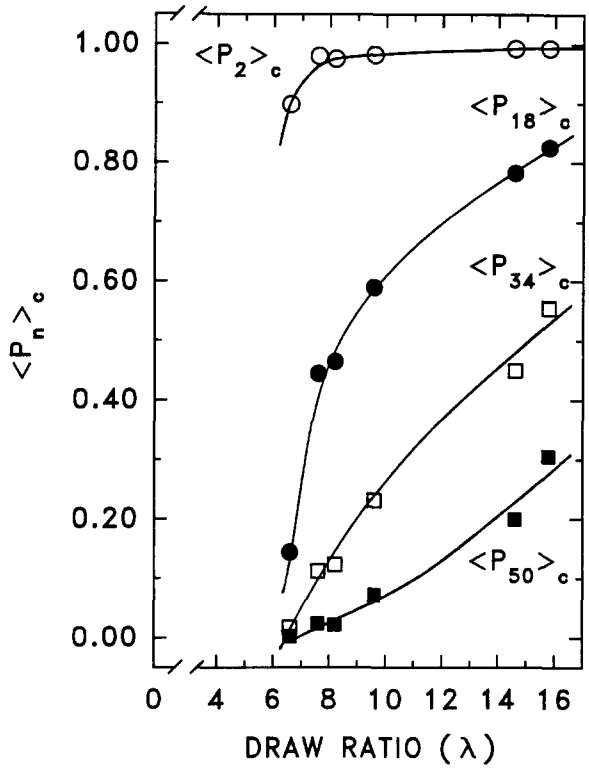

Figure 7 Selected $\langle P_n \rangle_c$ coefficients as a function of draw ratio for roll-drawn polypropylene sheets

Table 3 Selected $\langle P_n \rangle_c$ coefficients calculated for the 110 crystal planes of the $\lambda = 15.8$ polypropylene sheet, using different integration ranges in equation (2)

Integration range (χ)	$\langle P_2 \rangle_c$	$\langle P_{18} \rangle_c$	$\langle P_{34} \rangle_c$	$\langle P_{50} \rangle_c$
35°–90°	0.991	0.808	0.536	0.295
60°–90°	0.994	0.810	0.536	0.296
80°–90°	0.996	0.819	0.541	0.300

gets close to unity at $\lambda = 8$ and remains constant afterwards. However, the curves obtained for the higher order coefficients clearly show the increase of the molecular orientation in the most highly oriented samples studied in this work.

The results presented in *Figures 6* and *7* compare well with those obtained from X-ray measurements of the orientation in high-density polyethylene[15,16]. Previous studies have shown that the orientation of the crystalline phase of ultra-high-molecular-weight PE still increases at $\lambda \geqslant 50$, even if the $\langle P_2 \rangle_c$ coefficient gets to unity at extension ratios around 8–10. For polyethylene, it has been reported that the transformation from the lamellar to the fibrillar morphology is completed at such draw ratios[4]. It can therefore be proposed that the high-order $\langle P_n \rangle_c$ coefficients are necessary for the characterization of the highly oriented structure of stretched polymers which possess a fibrillar structure.

The usefulness of high-order $\langle P_n \rangle_c$ coefficients for the characterization of the crystal phase of highly oriented polymer samples can also be demonstrated by referring to a study of stretched polypropylene films made by Desper[10]. For highly oriented samples, this author underlines the fact that a significant decrease of the width of the orientation distribution causes only a small variation of the $\langle P_2 \rangle_c$ values. Desper reported that the $\langle P_2 \rangle_c$ coefficient increases only from 0.9917 to 0.9968 for samples where the $\chi_{1/2}$ value decreases by a factor of two, from 6.6° to 3.4° for the 110, 040 and 130 reflections. By comparison, the narrowing of the molecular orientation distributions from 6.8° to 4.2°, between the sheets with $\lambda = 9.6$ and 15.8 studied in the present work, results in significant increases of the high $\langle P_n \rangle_c$ coefficients, as is seen by comparing *Figures 6* and *7*.

Minor differences, as calculated by Desper for the $\langle P_2 \rangle_c$ coefficient, can also arise from calculation artefacts. *Table 3* gives selected $\langle P_n \rangle_c$ coefficients calculated for the 110 polar scan of the $\lambda = 15.8$ sheet by using different integration ranges in equation (2). The 35°–90° interval was chosen in order to exclude the contribution from the weak 001 reflection, whereas cutting between 35° and 60° further subtracts experimental noise in this region of the polar scan curve. Finally, calculations were made in the 80°–90° interval in order to compare with the results of Desper, although the tail of the orientation distribution is excluded in this restricted range. It is observed that the presence of noise in the background of the 110 scan, between 35° and 60°, can decrease the second-order coefficient from 0.994 to 0.991, whereas placing the integration limit at 80° instead of 35° leads to an increase in $\langle P_2 \rangle_c$ from 0.991 to 0.996. The discrepancy shown in *Table 3* between the higher-order coefficients obtained in different angular ranges is comparable, in absolute value, to that between the $\langle P_2 \rangle_c$ coefficients. However, the curves presented in *Figures 6* and *7* show that these variations are small in comparison with the increase of the high $\langle P_n \rangle_c$ coefficients that results from a decrease of the width of the orientation distribution.

CONCLUSIONS

In this work, $\langle P_n \rangle_c$ coefficients characterizing the molecular chain orientation were calculated from wide-angle X-ray diffraction measurements made on roll-drawn i-PP samples. The agreement between the results obtained from different crystal planes is excellent when contributions from unresolved reflections are removed by a curve-fitting procedure prior to the $\langle P_n \rangle_c$ calculations. The hot roll-drawing process induces double orientation in the samples, although this effect is small and the deviation from the cylindrical symmetry does not show up in the molecular chain orientation calculations. The $\langle P_2 \rangle_c$ and $\langle P_4 \rangle_c$ coefficients reach their limiting value of unity at $\lambda = 8$, indicating that the chains are highly oriented in the deformation direction at this draw ratio. However, the higher order $\langle P_n \rangle_c$ coefficients continue to increase up to $\lambda > 15$, which demonstrates that the use of these coefficients provides a reliable method to follow the evolution of the crystal phase orientation in highly oriented polymers.

ACKNOWLEDGEMENTS

This work was made possible through financial support from the Natural Sciences and Engineering Research Council of Canada and the Department of Education of the Province of Québec (FCAR and Actions Structurantes programmes). The authors also wish to thank Dr Raymond T. Woodhams of the University of Toronto

(Ontario, Canada) for providing the polypropylene sheets studied in this work.

REFERENCES

1 Ward, I. M. (ed.) 'Structure and Properties of Oriented Polymers', Applied Science Publishers, London, 1975
2 Ciferri, A. and Ward, I. M. (eds) 'Ultra-High Modulus Polymers', Applied Science Publishers, London, 1979
3 White, J. L. and Spruiell, J. E. *Polym. Eng. Sci.* 1983, **23**, 247
4 Peterlin, A. *Colloid. Polym. Sci.* 1987, **265**, 357
5 Wilchinsky, Z. W. *J. Appl. Phys.* 1960, **31**, 1969
6 Wilchinsky, Z. W. *J. Appl. Polym. Sci.* 1963, **7**, 923
7 Okajima, S., Kurihara, K. and Homma, K. *J. Appl. Polym. Sci.* 1967, **11**, 1703
8 Okajima, S. and Homma, K. *J. Appl. Polym. Sci.* 1968, **12**, 411
9 Samuels, R. J. *J. Polym. Sci. A-2* 1968, **6**, 1101
10 Desper, C. R. *J. Macromol. Sci.-Phys.* 1973, **B7**, 105
11 Dhingra, V. J., Spruiell, J. E. and Clark, E. S. *Polym. Eng. Sci.* 1981, **21**, 1063
12 Shimomura, Y., Spruiell, J. E. and White, J. L. *J. Appl. Polym. Sci.* 1982, **27**, 2663
13 Unwin, A. P., Bower, D. I. and Ward, I. M. *Polymer* 1985, **26**, 1605
14 Shankernarayanan, M. J. *PhD Thesis* University of Pittsburgh, PA, USA, 1986
15 Lafrance, C. P., Pézolet, M. and Prud'homme, R. E. *Macromolecules* 1991, **24**, 4948
16 Lafrance, C. P., Debigaré, J. and Prud'homme, R. E. *J. Polym. Sci., Polym. Phys. Edn* 1993, **31**, 255
17 Burke, P. E., Weatherly, G. C. and Woodhams, R. T. *Polym. Eng. Sci.* 1987, **27**, 518
18 Tate, K. R., Perrin, A. R. and Woodhams, R. T. *Polym. Eng. Sci.* 1988, **28**, 1264
19 Krigbaum, W. R. and Roe, R. J. *J. Chem. Phys.* 1964, **41**, 737
20 Tallqvist, H. *Acta Soc. Sci. Fenn., Ser. A* 1938, **II**, 2
21 Gupta, V. B. and Ward, I. M. *J. Macromol. Sci. Phys.* 1970, **B4**, 453
22 Desper, C. R., Southern, J. H., Ulrich, R. D. and Porter, R. S. *J. Appl. Phys.* 1970, **41**, 4284
23 Lovell, R. and Mitchell, G. R. *Acta Crystallogr.* 1981, **A37**, 135
24 Natta, G. and Corradini, P. *Nuovo Cimento, Suppl.* 1960, **15**, 40
25 Turner-Jones, A., Aizlewood, J. M. and Beckett, D. R. *Makromol. Chem.* 1964, **75**, 134
26 Stanisz, G. J., Holender, J. M. and Soltys, J. *Powder Diffract.* 1989, **4**, 70
27 Heuvel, H. M., Huisman, R. and Lind, K. C. J. B. *J. Polym. Sci., Polym. Phys. Edn* 1976, **14**, 921
28 Sajkiewicz, P. and Wasiak, A. *J. Appl. Crystallogr.* 1990, **23**, 88